

Special Section:

Significant advances in ocean and climate sciences of the Pacific-Asian Marginal Seas

Key Points:

- The Mindanao Current (MC) transport variability is inferred using the tide gauge sea level data at Malakal and Davao
- MC variability was dominated by biennial oscillations in 1970s, interannual fluctuations in 1980s, and decadal variability after 1990s
- Similar biennial→interannual→decadal transitions were detected in the surface wind stress curl field over the western tropical Pacific

Correspondence to:

X. Chen,
chenxiao1231@hhu.edu.cn





Citation:

Chen, X., Qiu, B., Chen, S., & Qi, Y. (2021). Period-lengthening of the Mindanao Current variability from the long-term tide gauge sea level measurements. *Journal of Geophysical Research: Oceans*, 126, e2020JC016932. <https://doi.org/10.1029/2020JC016932>

Received 14 NOV 2020

Accepted 13 JUL 2021

Period-Lengthening of the Mindanao Current Variability From the Long-Term Tide Gauge Sea Level Measurements

Xiao Chen^{1,2} , Bo Qiu³ , Shuiming Chen³ , and Yiquan Qi¹ 

¹College of Oceanography, Hohai University, Nanjing, China, ²Southern Marine Science and Engineering Guangdong Laboratory (Zhuhai), Zhuhai, China, ³Department of Oceanography, University of Hawaii at Manoa, Honolulu, HI, USA

Abstract Long-term tide gauge sea level data from 1969 to 2014 at Davao (7.08°N, 125.63°E) and Malakal (7.33°N, 134.46°E) are analyzed to examine the decadal frequency modulations embedded in the Mindanao Current (MC) variability. The MC variability inferred from the Davao–Malakal sea level was predominantly biennial in the 1970s. This prevailing period switched to interannual in the 1980s and lengthened to decadal during the last two decades. With the aid of the basin-scale sea level information from satellite altimeter measurements, it is found that the sea level-inferred MC variability represents the coherent changes of the wind-driven tropical gyre in the western North Pacific. An investigation into the long-term wind stress curl data reveals that its prevailing period underwent similar biennial→interannual→decadal transitions in the western tropical Pacific, implying the forced nature of the period-lengthening of the MC variability during the past half-a-century. While the sign of the MC variability is largely determined by the Malakal sea level signals on the interannual and decadal time scales, the Davao sea level change becomes important when the time scale extends to multi-decades.

Plain Language Summary Flowing southward along the Philippine coast from 13°N to 5°N, the Mindanao Current (MC) is a western boundary current and serves to close the wind-driven tropical gyre in the North Pacific Ocean. Climatically, the MC plays a critical role by transporting the mid-latitude North Pacific water equatorward with a portion of it entering the eastern equatorial Pacific Ocean and contributing to the upper ocean heat budget in the cold-tongue region. The other portion of the MC permeates into the Eastern Indian Ocean via the Indonesian Throughflow and facilitates the water mass/heat exchange between the Pacific and Indian Oceans. Despite its importance, observations of the MC transport have been rare and our understanding of its long-term variability is lacking. By utilizing the available tide gauge data at Davao and Malakal across the MC, we explored the MC transport variability of the past half-a-century. It is found that the timescale of the MC transport change has lengthened since 1969. While 2-year-period oscillations dominated in the 1970s, 4 ~ 6-year-period fluctuations took over during the 1980s, and the decadal variability became pre-dominant after 1990s. The cause behind these changes in timescale is due to the similar changes in the tropical Pacific surface wind system that ultimately drives the MC.

1. Introduction

Forced externally by both basin-scale trade winds and regional monsoonal winds of the Maritime Continent, the western tropical Pacific Ocean is where many major low-latitude oceanic currents originate, bifurcate, and interact. In the Northern Hemisphere, the North Equatorial Current (NEC) flows westward, carrying wind-driven convergent Sverdrup transport across the interior Pacific (Figure 1a). After reaching the Philippine coast, the NEC bifurcates into the northward-flowing Kuroshio and the southward-flowing Mindanao Current (MC; Wijffels et al., 1995; Qiu & Lukas, 1996; Zhang et al., 2014). Part of the MC intrudes into the Celebes Sea and feeds the Indonesian Throughflow (ITF), and the remaining part veers eastward to form the North Equatorial Countercurrent (NECC; Gordon & Fine, 1996; Hsin & Qiu, 2012; Kashino et al., 2005; Lukas et al., 1991). As is typical for a western boundary current outflow, the NECC is known to exhibit stationary meanders that are accompanied by two permanent recirculating eddies: the cyclonic

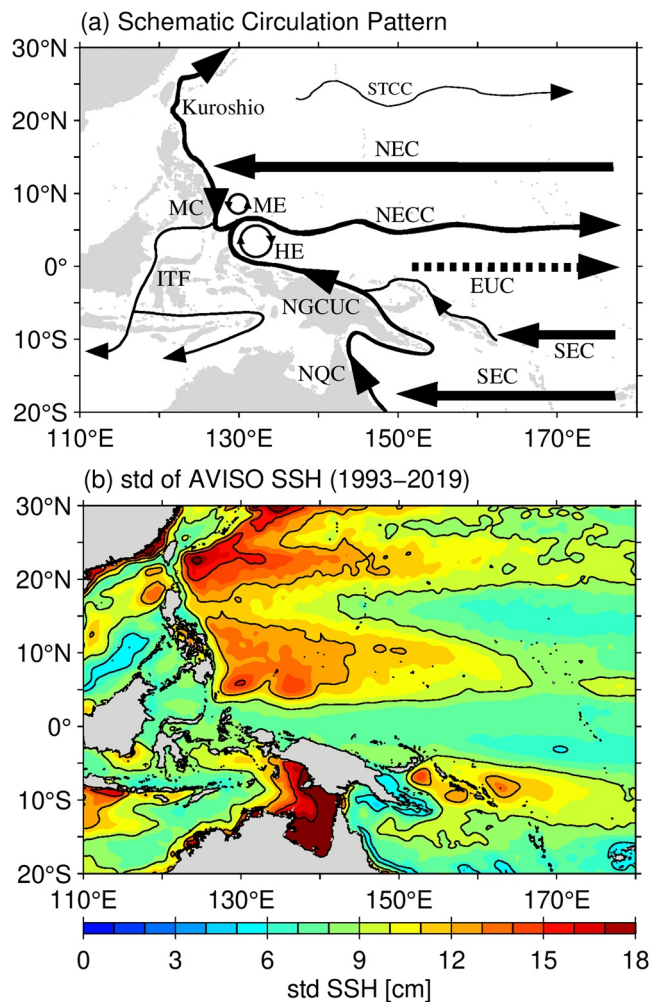


Figure 1. (a) Upper ocean circulation schematic in the western tropical Pacific Ocean. Currents shown are: Subtropical Countercurrent (STCC); North Equatorial Current (NEC); Mindanao Current (MC); Mindanao Eddy (ME); North Equatorial Countercurrent (NECC); Halmahera Eddy (HE); Indonesian Throughflow (ITF); Equatorial Undercurrent (EUC); New Guinea Coastal Undercurrent (NGCUC); South Equatorial Current (SEC); and North Queensland Current (NQC). (b) Sea surface height standard deviation map based on AVISO merged satellite altimeter data of 1993–2019.

Mindanao Eddy (ME) centered around 7.5°N, 128°E and the anticyclonic Halmahera Eddy (HE) centered near 38°N, 131°E (Chen et al., 2015; Heron et al., 2006; Kashino et al., 2013).

As indicated by the sea surface height (SSH) standard deviations shown in Figure 1b, the oceanic currents in the tropical western Pacific are dynamically highly variable. This is so because not only are they influenced by the regional monsoonal wind forcing and intrinsic instabilities, they are also subject to the perturbations originating in the interior Pacific basin due to the planetary β effect. Climatically, the upper ocean circulation variations play important roles in mass and heat budget/balance in the western tropical Pacific and in regulating the warm pool evolution and the life cycle of ENSO. For example, the time-varying MC can affect the convergent surface warm water of the warm pool to the east and it can also modify the ITF transport through its intrusion into the Celebes Sea (e.g., Chen et al., 2018; Kashino et al., 2001; Qiu et al., 1999). A comprehensive recent review on both regional and global climate by the western tropical Pacific Ocean variability can be found in Hu et al. (2015).

Exploring the long-term circulation variability in the western tropical Pacific Ocean, such as the MC, has been challenging due to lack of sustained in-situ measurements. As such, many investigators of the MC variability in the past have relied on analyses of numerical model simulations (e.g., Chen & Wu, 2011; Chen et al., 2016; Duan et al., 2019a, 2019b; Kim et al., 2004). Observationally, one effective way to monitor the long-term western boundary current variability is to utilize the tide gauge sea level measurements. Due to the strong constraint by geostrophy, sea level difference across a western boundary current has been utilized widely to infer its transport fluctuations. In the subtropical western North Pacific, for example, Chang and Oey (2011) used the tide gauge sea level difference between Keelung and Ishigaki to infer the Kuroshio transport variations east of Taiwan. Similarly, Kawabe (1995) explored the Kuroshio transport fluctuations across the Tokara Strait by using the tide gauge sea level data between Naze and Nishinoomote. For the MC variability, by using the sea level data measured at Davao and Malakal tide gauges, Lukas (1988) observed that, for the analysis period of 1974–1985, the MC transport was dominated by interannual variations with a quasi-biennial period. This pioneering work by Lukas (1988) has motivated several succeeding investigations into the ocean-atmosphere-land interactions in the low-latitude western Pacific that generate alternating strong and weak Asian monsoons with the quasi-biennial surface wind fluctuations (e.g., Barnett, 1991; Masumoto & Yamagata, 1991; Meehl, 1987; Tozuka et al., 2002; Yasunari, 1989).

With the changing climate in the tropical Pacific Ocean in recent decades (e.g., Merrifield, 2011; Qiu & Chen, 2012; Vecchi et al., 2006; Tokinaga et al., 2012), a question arising naturally is whether the quasi-biennial variations detected in 1974–1985 in the sea level-inferred MC variability remained as a dominant signal after 1985. Fortunately, sea level measurements have been continuously conducted at Davao and Malakal tide gauge after the mid 1980s. With the advent of satellite altimeter measurements since late 1992, we have now further a spatially homogeneous, global sea level data set that allows us to examine the tide gauge-derived results in a broader context of the regional circulation variations. By using these observationally enhanced sea level information, we seek in this study to clarify the long-term modulations of the MC variability and their connections to the Pacific basin-wide surface wind forcing over the past half century.

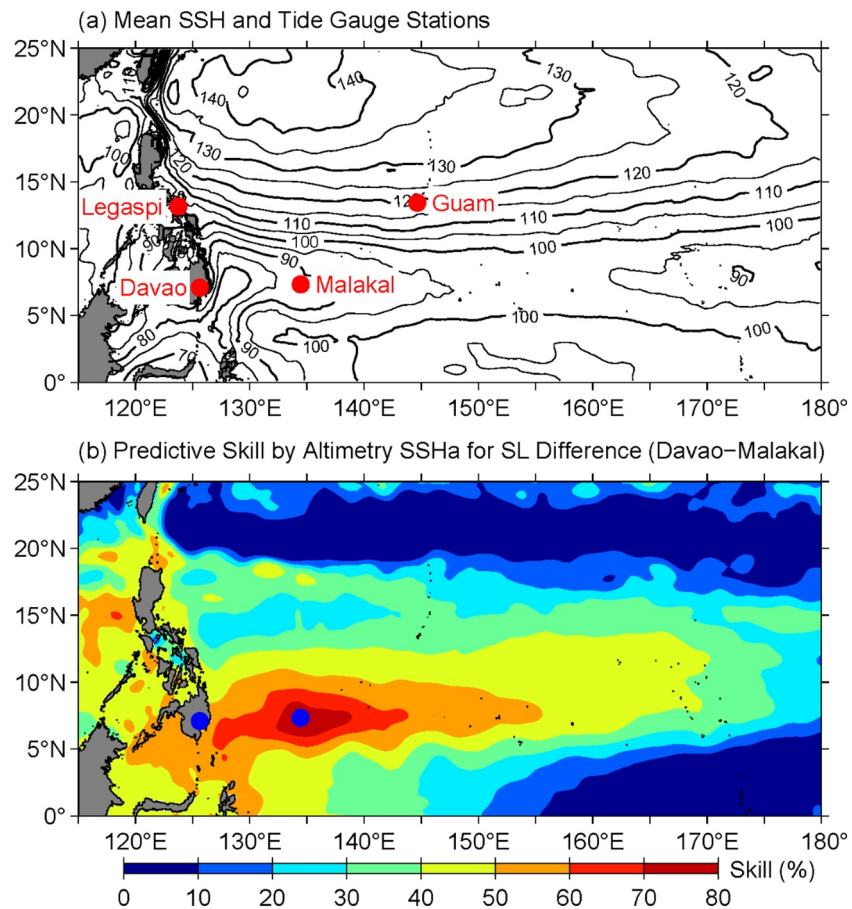


Figure 2. (a) Mean sea surface height (cm) in the tropical northwestern Pacific Ocean from Rio et al., (2011). Red dots denote the locations of the four tide gauge stations analyzed in this study. (b) Percentage of variance explained by the AVISO sea surface height anomaly signals for the sea level difference time series of Davao minus Malakal in the period of 1993–2014.

2. Data

The present study uses three data sources: tide gauge sea level measurements, gridded satellite altimeter data set, and atmospheric reanalysis product for surface wind stresses. The data analysis covers the period of past 56 years from 1959 to 2014. For the long-term sea level data from Malakal (7.33°N, 134.46°E) and Guam (13.43°N, 144.65°E; see Figure 2a for their locations), we use the daily research-quality product archived by the University of Hawaii Sea Level Center (UHSLC; <http://uhslc.soest.hawaii.edu>). For the long-term sea level data at Davao (7.08°N, 125.63°E) and Legaspi (13.15°N, 123.75°E) after 1983, we again use the daily UHSLC research-quality product. Occasional sea level time series gaps appear at these two coastal tide gauge stations and they are filled by using the satellite altimetry-derived AVISO sea level product (<http://www.aviso.oceanobs.com>). For the Davao and Legaspi sea level data prior to 1983, we utilize the monthly sea level time series compiled by the Permanent Service for Mean Sea Level (<http://www.psmsl.org>; Woodworth & Player, 2003). Available sea level data started from 1969 at Malakal and, at the other three tide gauge stations, we used 1959 as the starting date. The global AVISO sea level product is available from 1993.

For the long-term surface wind stress data, we adopt the European Center for Medium-Range Weather Forecasts (ECMWF) interim monthly product of 1979–2014 (<http://apps.ecmwf.int>; Dee et al., 2011). For the period of 1959–1978, the monthly wind stress time series is supplemented by the ECMWF Ocean Analysis System ORA-S3 product (<http://apdrc.soest.hawaii.edu>; Balmaseda et al., 2008). The ECMWF interim and ORA-S3 wind stress products have a spatial resolution of $0.75^\circ \times 0.75^\circ$ and $1^\circ \times 1^\circ$, respectively, and in the tropical Pacific Ocean of our interest, they match favorably in their overlapping period of 1979–2012.

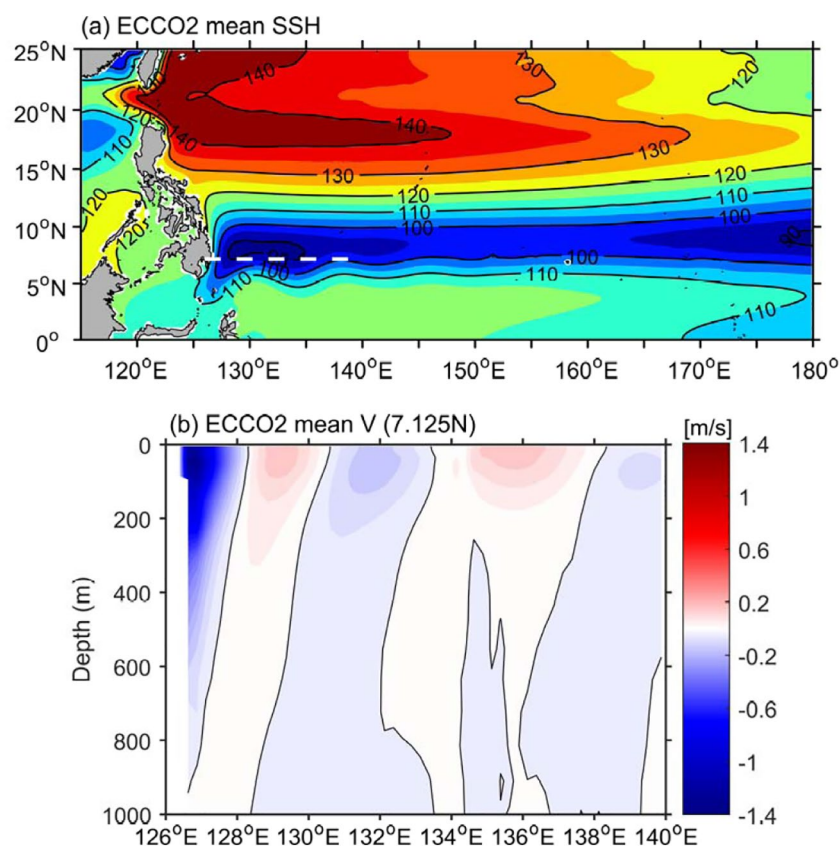


Figure 3. (a) Mean sea surface height (cm) in the tropical northwestern Pacific Ocean from the ECCO2 state estimates. (b) Mean ECCO2 meridional velocity profile along 7.125°N from the Philippine coast to 140°E, that is, the red dashed line in (a).

3. MC Transport Variability Versus Davao–Malakal Sea Level

Although the sea level difference between Davao and Malakal has been used by Lukas (1988) to infer the MC transport changes, the fidelity of this inference and the relationship between the Davao–Malakal sea level and MC transport changes have not been previously established. In order to examine the fidelity and establish the relationship, we use in this study the ocean state estimate product from the Estimating the Circulation and Climate of the Ocean, Phase II (ECCO2). The ECCO2 simulation is based on the three-dimensional hydrostatic and Boussinesq Massachusetts Institute of Technology general circulation model (Marshall et al., 1997). The model has a mean horizontal resolution of 18 km and 50 vertical levels with varying resolution from 10 m near the surface to 456 m near the ocean bottom. The eddy-permitting ocean state estimate is obtained by a least squares fit of the model to available satellite observations and in situ measurements. Using the optimized parameters, such as the initial temperature-salinity conditions, eddy diffusivity and viscosity, surface boundary conditions, and bottom drags, based on a Green's function approach (Menemenlis et al., 2005), the ECCO2 model is run unconstrained as in prognostic model simulations. As no observational data are imposed in the forward integration, the ECCO2 output is considered to be dynamically consistent (Wunsch et al., 2009). This point is important to our study as the sea level and MC changes are dynamically constrained consistently in the ECCO2 product.

Figure 3a shows the mean sea surface height field of 1994–2018 simulated by ECCO2 in the western tropical Pacific Ocean. Consistent with our recent study focus on the Celebes Sea circulation variability (Chen et al., 2018), it compares well with the time-mean sea surface height map derived from the satellite altimetry and other in-situ measurements shown in Figure 2a. In Figure 3b, we plot the mean meridional velocity profile along 7.125°N from the Philippine coast to 140°E from the ECCO2 simulation. The simulated mean MC, which can be identified as the strong southward boundary current appearing west of 128.3°E against

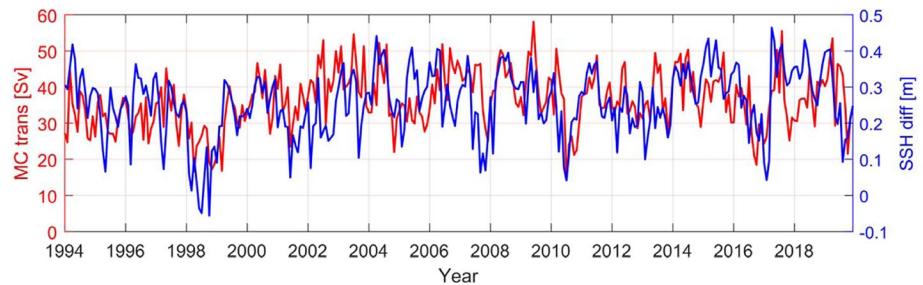


Figure 4. Monthly time series of the southward-flowing Mindanao Current transport (red line) versus the Davao–Malakal sea surface height difference (blue line) from the ECCO2 state estimates.

the Philippine coast, has a transport of 36.5 Sv. This transport value agrees well the 36.1 Sv value derived from the repeat glider measurements across $\sim 8^{\circ}\text{N}$ (Schönau et al., 2015). Vertical structure-wise, the simulated MC tilts westward with increasing depth, a feature in close agreement with the observed time-mean MC from repeat hydrographic surveys (Wijffels et al., 1995; their Figure 5b) and repeat glider measurements (Schönau et al., 2015; their Figure 2a). East of 128.3°E , Figure 3b reveals the presence of oscillatory meridional mean velocities and, as indicated in Figure 3a, these velocities correspond to the observed stationary meanders of the NECC (Heron et al., 2006; Hsin & Qiu, 2012; Lukas et al., 1991; Zhao et al., 2013).

To examine how the MC transport variability is related to the sea level difference between Davao and Malakal, we compare in Figure 4 the monthly time series between the MC transport (red line) and the sea level difference between Davao and Malakal (blue line) based on the ECCO2 state estimates. Here, the MC transport is calculated by integrating the southward meridional velocity from the Philippine coast to 129°E . By and large, the two time series show good correspondence and have a linear correlation coefficient $R = 0.41$. With the decorrelation timescale of the two time series estimated at 4 months and the degree of freedom of the time series at 39 (13 years \times 12 months/yr/4 months), this R value is statistically significant at the 99% confidence level. Note that this R value increases to 0.57 if a low-pass filter is applied to the two time series in Figure 4 to retain only the interannual signals. Given this comparison, we believe the tide gauge sea level data from Davao and Malakal can be used effectively for evaluating the transport changes of the MC. Quantitatively, the result of Figure 4 suggests that a sea level difference change of 0.1 m corresponds to a 10 Sv change in the MC transport.

4. Results of Tide Gauge Data Analysis

Figures 5a and 5b show the time series of sea level anomalies observed at Davao and Malakal, respectively; gray lines denote the original monthly time series and red lines are the low-pass filtered time series. Here, the Gaussian low-pass filter has a form of $\exp(-d^2 / 2\sigma^2)$, where d is the temporal separation and $\sigma = 100$ days. Visually, the time-varying sea level signals at Malakal exhibit larger amplitudes than those at Davao. To quantify their frequency contents as a function of time, we plot in Figures 6a and 6b the wavelet power spectra of the Davao and Malakal sea level time series, respectively. Both wavelet power spectra reveal similar temporal evolutions: the biennial fluctuations dominated in the 1970s, the interannual signals with period of 3–6 years became prevalent in the 1980s, and the decadal fluctuations took over during the last two decades. Consistent with the visual inspection, the wavelet power spectral level in all time and frequency bands appears higher at the offshore Malakal than at Davao on the Philippine coast. This tide gauge-derived result is also concordant with the satellite altimeter-measured sea surface height standard deviation pattern (Figure 1b) that shows the SSH standard deviation is ~ 8 cm along the Philippine coast versus ~ 16 cm surrounding Palau.

The biennial \rightarrow interannual \rightarrow decadal transitions seen in the sea level data at Malakal and Davao become even more prominent when we take the sea level difference of Davao minus Malakal (Figures 5c and 6c). In accordance with the findings by Lukas (1988), biennial fluctuations were conspicuously regular during 1972–1983, with higher Davao–Malakal sea level (i.e., an intensified MC) occurring in 1972, 1974, 1976, 1978, 1980, and 1982, respectively. These biennial signals, however, ceased to exist after 1984 and, in the

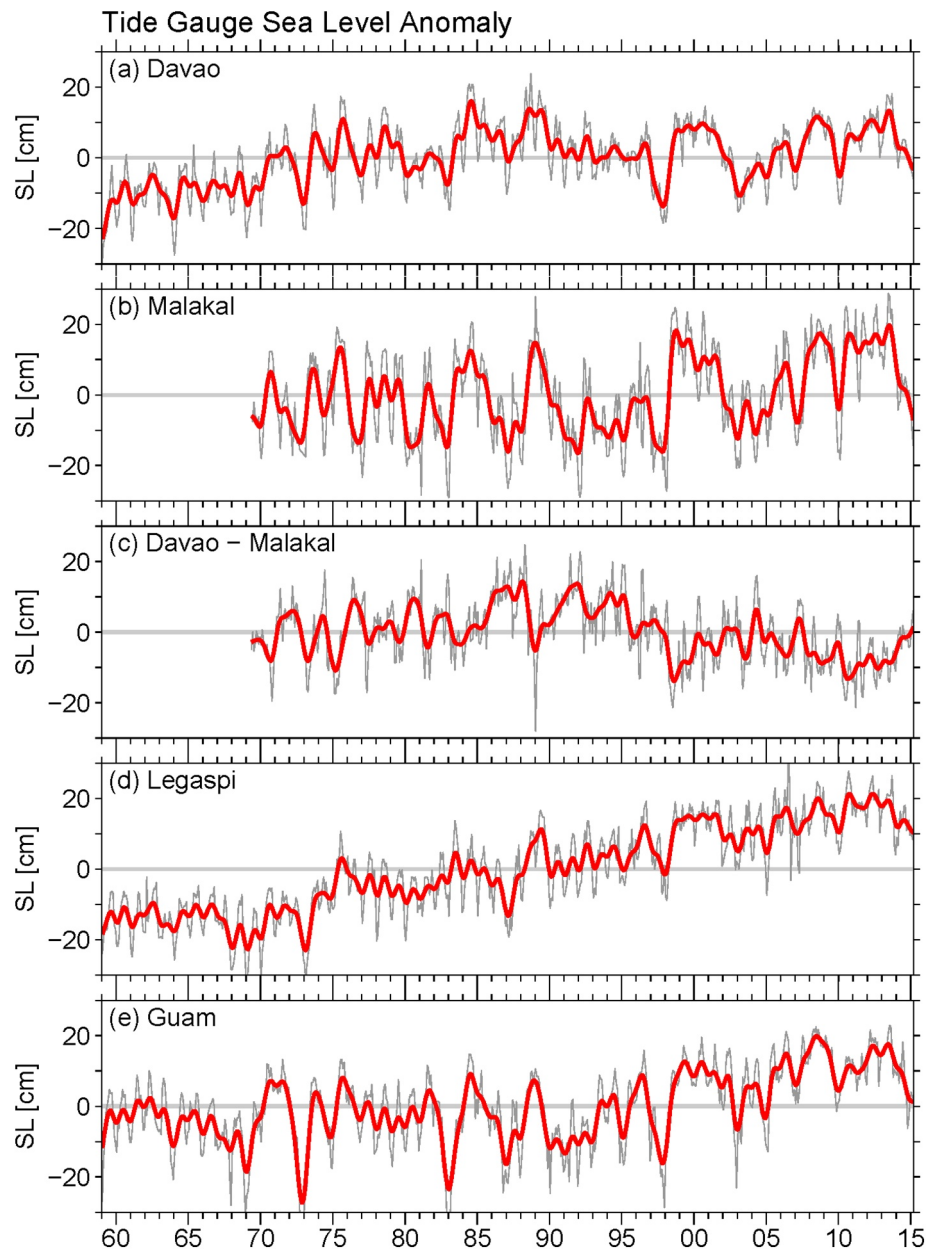


Figure 5. Time series of the observed sea level anomalies at (a) Davao, (b) Malakal, (c) Davao minus Malakal, (d) Legaspi, and (e) Guam. Gray and red lines denote the monthly and low-pass filtered time series, respectively. Tick marks in x-axis correspond to January of individual years.

subsequent decade, the sea-level-inferred MC intensified in 1986/87, 1991/92 and 1994/95, respectively. During the last two decades, the Davao-Malakal sea level revealed a longer-period oscillation and, at the same time, there emerged enhanced variance with an annual period. As can be discerned in Figure 3c, in terms of the phase of the annual cycle, a larger (smaller) sea level difference between Davao and Malakal tends to appear in March–May (October–December). Notice that this seasonal change in MC's intensity agrees with the existing studies focusing on the MC seasonality (e.g., Kashino et al., 2005; Chen et al., 2015; Schönau & Rudnick, 2017).

It is important to emphasize that the biennial→interannual→decadal transitions in sea level variability after 1970 are not unique to the Malakal and Davao tide gauge stations. An examination into the long-term sea level time series from other tropical western Pacific Ocean, for example, at Legaspi and Guam, reveals

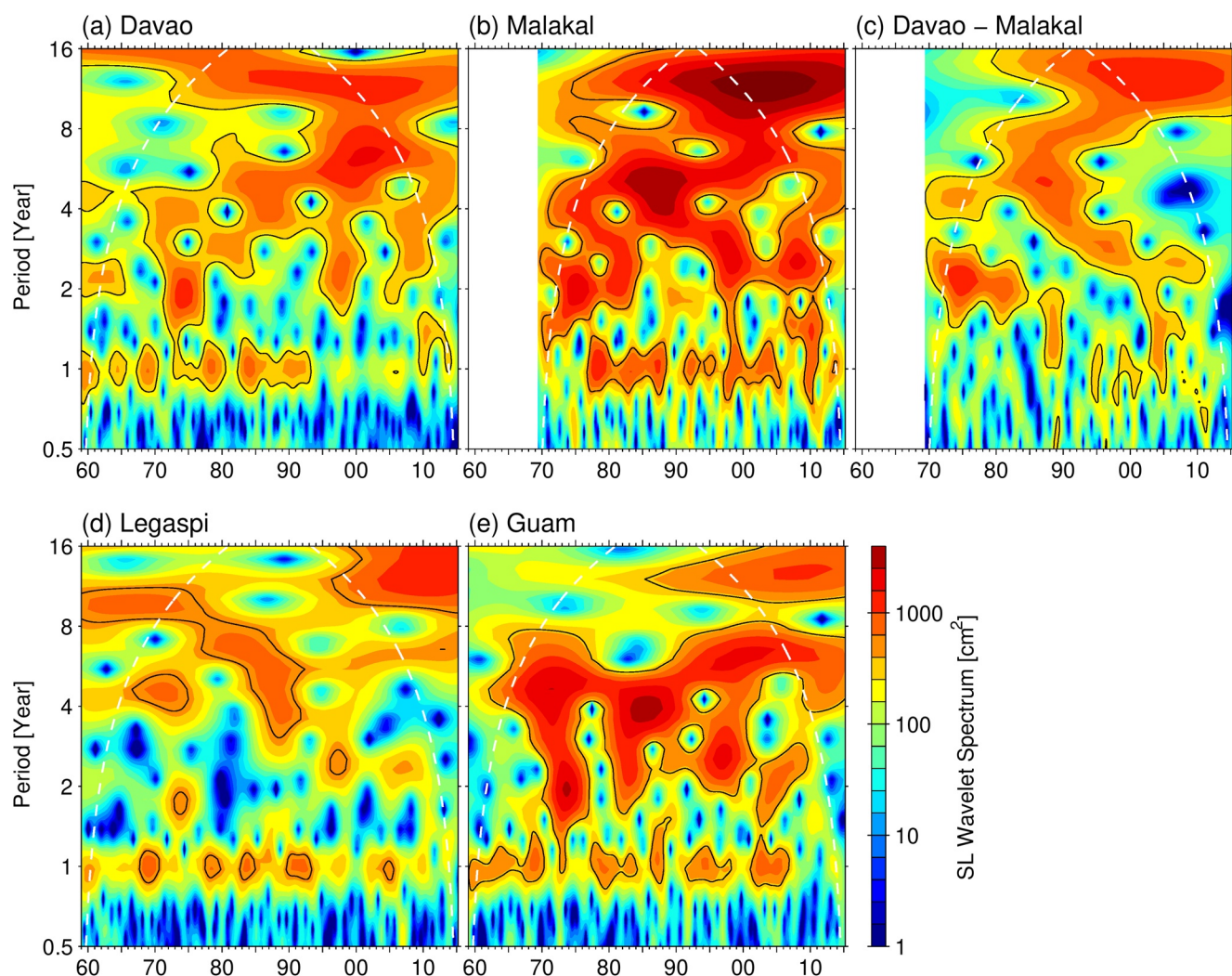


Figure 6. Wavelet power spectra for the observed sea level anomalies at (a) Davao, (b) Malakal, (c) Davao minus Malakal, (d) Legaspi, and (e) Guam. Dashed lines in all plots indicate cones of influence by the edge effects. Black contours denote the 95% confidence levels based on Torrence and Compo (1997). Tick marks in x-axis correspond to January of individual years.

similar transitions in the dominating periods over the past 56 years (see Figures 5d–5e and 6d–6e). The biennial→interannual→decadal transitions, however, are absent in the long-term sea level time series from the western Pacific tide gauge stations north of 20°N. For example, Figures 7a and 7b show the sea level time series and its wavelet power spectra at Ishigaki (24.33°N, 124.15°E), a tide gauge station representative of the sea level changes in the subtropical western North Pacific Ocean. The sea level signals there are dominated by seasonal fluctuations and the decadal modulating interannual variability. Less variance is detected in the biennial and decadal frequency bands when compared to the tide gauge stations in the tropical western North Pacific Ocean. This comparison clearly points to the tropical nature of the biennial→interannual→decadal transitions in the time-varying sea level field.

5. Discussion and Summary

To provide a broad-scale context to the sea-level-inferred MC variability, it is instructive to use the global AVISO sea level data set and examine the connection between the Davao–Malakal sea level signals and those in the broader region of the tropical western Pacific Ocean. Figure 2b shows the percentage of variance of the Davao–Malakal sea level time series $P(t)$ (i.e., the red line in Figure 5c) explained by the sea level time series $Q(t)$ at other locations of the western Pacific Ocean:

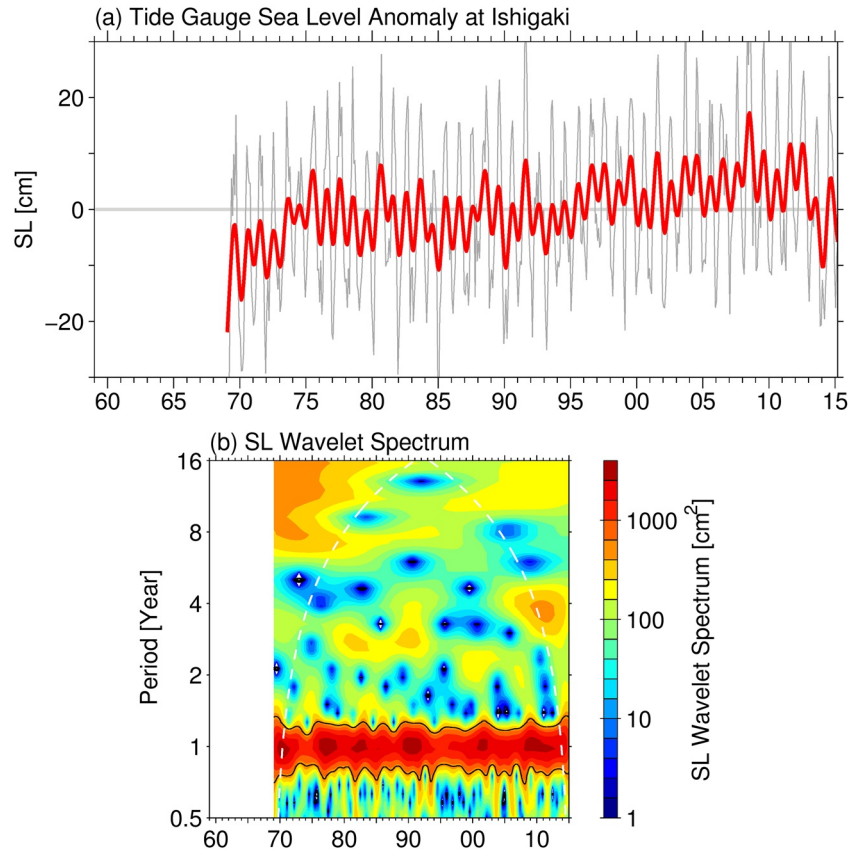


Figure 7. (a) Time series of the observed sea level anomalies at Ishigaki. Gray and red lines denote the monthly and low-pass filtered time series, respectively. (b) Wavelet power spectrum for the observed sea level anomalies at Ishigaki. Dashed lines in (b) indicate cones of influence by the edge effects and black contours denote the 95% confidence levels. Tick marks in x-axis correspond to January of individual years.

$$s = 1 - \frac{\langle [Q(t) - P(t)]^2 \rangle}{\langle P^2(t) \rangle}, \quad (1)$$

where $\langle \rangle$ denote time averaging over the period of 1993–2014. Due to the dominance of the sea level signals at Malakal over those at Davao, it is not surprising to see the highest variance ($s = 75.2\%$) is explained by the Malakal sea level signals. Rather than confined to a small area surrounding Malakal, however, Figure 2b reveals that the area with high values of explained variance extends to a broad region of the wind-driven North Pacific tropical gyre. In fact, the shape of the $s = 40\%$ contours in Figure 2b follows the 100-cm mean SSH contours that delineate the time-mean wind-driven tropical gyre in Figure 2a quite well. Physically, this implies that the low-frequency MC variability inferred from the Davao–Malakal sea level is not determined by local processes, but is controlled by the broad-scale surface wind forcing over the tropical Pacific basin.

Many existing studies in the past have demonstrated that the low-frequency sea level fluctuations in the western tropical Pacific Ocean are controlled by the wind stress curl forcing through baroclinic Rossby wave adjustment processes (see Qiu & Chen, 2012 for references and a quantitative evaluation). To relate the frequency transitions in the MC variability to the basin-scale surface wind forcing field, we plot in Figure 8a the wind stress vector and curl field regressed to the normalized, low-pass filtered Davao–Malakal sea level time series of 1969–2014. In accordance with the previous study of the decadal NEC variability along the Philippine coast (Qiu & Chen, 2010), large-amplitude positive curl signals are seen along the 7°–15°N band in the western Pacific basin. With the MC being the compensating boundary current driven by the positive wind stress curls, or Ekman suction, in the tropical gyre, this regression pattern of the positive interior curl values is consistent with the Sverdrup dynamics, namely, an enhanced positive wind stress curl works to increase the western boundary current transport.

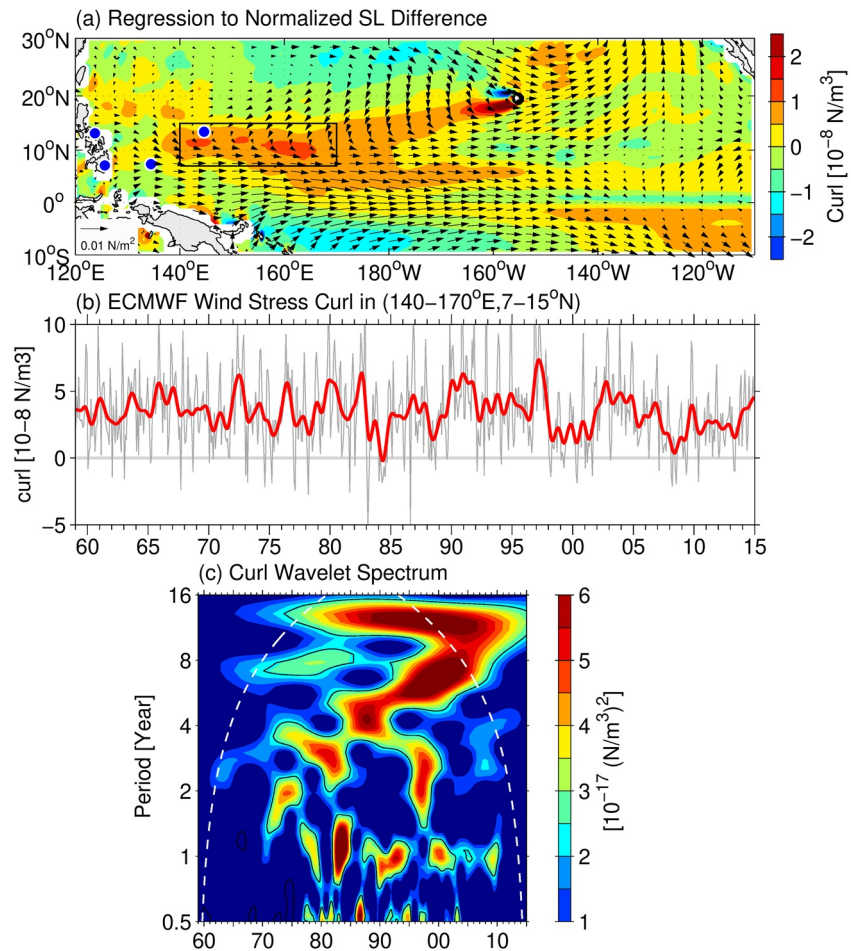


Figure 8. (a) Wind stress vector and curl regressed to the normalized, low-pass filtered, Davao–Malakal sea level difference time series shown in Figure 3c. (b) Monthly and low-pass filtered wind stress curl time series averaged in 7°–15°N and 140°–170°E. (c) Wavelet power spectrum for the monthly wind stress curl time series shown in (b). Dashed lines in (c) indicate cones of influence by the edge effects and black contours denote the 95% confidence levels. Tick marks in x-axis correspond to January of individual years.

In Figure 8b, we plot the monthly wind stress curl time series averaged in 7°–15°N, 140°–170°E where the regressed wind stress curl amplitude is large (see the box in Figure 8a). A look at the wavelet power spectrum for this wind stress curl time series (Figure 8c) reveals the same frequency transitions from biennial in the 1970s, to interannual in the 1980s, and to decadal in the last two decades, as detected for the Davao–Malakal sea level time series (recall Figure 6c). This correspondence indicates that it is the frequency transitions in the wind stress curl field over the western tropical Pacific Ocean that is responsible for the biennial→interannual→decadal MC variability as inferred from the Davao–Malakal sea level data. With respect to the enhanced variance in the annual Davao–Malakal sea level signals after the mid 1980s detected in Figure 6c, it is of interest to emphasize that a similar enhancement in the annual wind stress curl forcing is captured in Figure 8c. This reflects, again, the close connection between the frequency modulations in the surface wind forcing field and the resultant oceanic circulation variability in the western tropical Pacific Ocean.

Processes responsible for the frequency modulations in the tropical Pacific surface wind system of the past half century are likely due to the changing climate in the coupled ocean–atmosphere system (Hu et al., 2015; Tokinaga et al., 2012; Vecchi et al., 2006). For example, the dominance by the decadal variability in the recent 2–3 decades could be related to the enhanced influences from the Pacific mid-latitudes (e.g., England et al., 2014; Kosaka & Xie, 2013) and there are also possibilities that the tropical Pacific wind modulations are remotely induced from the Atlantic Ocean basin (e.g., Kucharski et al., 2011; Wu et al., 2019; and ref-

erences cited therein). Although clarifying those processes is beyond the scope of our present study, future studies are required that can elucidate the dynamical mechanisms underlying the long-term surface wind changes in the tropical western Pacific in general and the biennial→interannual→decadal transitions in particular.

In concluding this study, we briefly comment on the multi-decadal MC changes as measured by the Davao–Malakal sea level. Marked by a shift around 1988/89, Figure 5c shows that the Davao–Malakal sea level had an overall increasing trend at 5.1 mm/yr during the period of 1969–1988 and a decreasing trend at −6.1 mm/yr during 1989–2014. These trends are related to the multi-decadal Sverdrup circulation changes in the tropical Pacific Ocean. Specifically, in the period of 1969–1988, the southward Sverdrup transport along the western boundary of 6°–10°N calculated based on the ECMWF reanalysis had an increasing trend of 0.14 Sv/yr, and this trend is reversed to −0.07 Sv/yr during the period of 1989–2014. Notice that the ratio between the Sverdrup transport and Davao–Malakal sea level trends do not need to be a constant on multi-decadal timescales. In a 1.5-layer reduced-gravity model setting, for example, the Sverdrup transport trend V^t can be related to the sea level trend Δh^t via geostrophy by $V^t = (gH_0 / f) \Delta h^t$, where f is the Coriolis parameter, g the gravitational constant, and H_0 the mean upper layer thickness. The larger ratio of $V^t / \Delta h^t$ in 1969–1988 as compared to that in 1989–2014 implies that the mean upper layer thickness H_0 has a larger value in 1969–1988 (~494m) than in 1989–2014 (~207m). This long-term decrease in upper layer thickness is consistent with the increased upper ocean stratification since the 1960s observed in the tropical Pacific Ocean (see Yamaguchi & Suga, 2019, and the references therein).

It is worth noting that the 1969–1988 increasing and 1989–2014 decreasing trends in MC intensity identified from Figure 5c are opposite to the MC trends found by (Duan et al., 2019a, their Fig. 4; Duan et al., 2019b) based on an eddy-resolving OGCM, ocean state estimate products, and reduced-gravity model simulations. Our 1969–1988 increasing trend in MC intensity, on the other hand, is consistent with the MC trend found by Hu et al. (2021), their Figure 5b) based on historical hydrographic data. Also, our 1989–2014 decreasing trend in MC intensity is consistent with the studies that observed a southward shift trend in the NEC bifurcation along the Philippine coast (Qiu et al., 2015; Qiu & Chen, 2010; Wu et al., 2019). Regarding the connection between the long-term MC variability and the interior ocean wind forcing, we believe it is the zonally integrated wind stress curl (i.e., the Sverdrup transport), not the zonal-mean wind stress, that controls the MC transport in the tropical North Pacific gyre.

By examining the sea level time series at Davao and Malakal in Figures 5a and 5b, it is interesting to note that the increasing trend of the Davao–Malakal sea level during 1969–1988 is largely due to the increasing sea level at Davao (with a trend at 6.1 mm/yr). The Malakal sea level trend during this period remained largely flat at 0.4 mm/yr. This multi-decadal sea level trend difference between the interior ocean and Philippine coast tide gauges is also discernible in the Legaspi versus Guam sea level data, namely, the sea level rise trend prior to 1988/89 is more prominent at Legaspi than at Guam (cf., Figures 5d and 5e). In contrast, the recent decreasing trend of the Davao–Malakal sea level in 1989–2014 is caused mostly by the larger sea level rise at Malakal (7.4 mm/yr) than that at Davao (1.3 mm/yr). This result indicates that while the Malakal sea level signals dominate those of Davao for the sign of the MC variability on the interannual and decadal time series, the Davao sea level change becomes important when the time scale extends to multi-decadal. At present, the reason behind this multi-decadal shift in importance of the Philippine coastal sea level remains unclear and future studies are called for its further clarifications.

Data Availability Statement

The long-term tide gauge data can be assessed from the University of Hawaii Sea Level Center (<https://uhslc.soest.hawaii.edu/datainfo/>) and the Permanent Service for Mean Sea Level (<https://www.psmsl.org/data/>). The merged satellite altimeter data are from the CLS Space Oceanography Division as part of the Environment and Climate EU ENACT project (<http://www.aviso.oceanobs.com>). The surface wind stress data are from by European Center for Medium-Range Weather Forecasts (<http://apps.ecmwf.int>).

Acknowledgments

Constructive comments made by the two anonymous reviewer helped improve an early version of the manuscript. The long-term tide gauge data were provided by University of Hawaii Sea Level Center and the Permanent Service for Mean Sea Level, the merged satellite altimeter data by the CLS Space Oceanography Division as part of the Environment and Climate EU ENACT project, and the surface wind stress data by European Center for Medium-Range Weather Forecasts. This study is supported by the National Key R&D Program of China (2018YFA0605703), the National Natural Science Foundation of China (grant 41706004), the Natural Science Foundation of Jiangsu Province (grant BK20170872).

References

- Balmaseda, M. A., Vidard, A., & Anderson, D. L. T. (2008). The ECMWF ocean analysis system: ORA-S3. *Monthly Weather Review*, 136, 3018–3034. <https://doi.org/10.1175/2008mwr2433.1>
- Barnett, T. P. (1991). The interaction of multiple time scales in the tropical climate system. *Journal of Climate*, 4, 269–285. [https://doi.org/10.1175/1520-0442\(1991\)004<0269:tiomts>2.0.co;2](https://doi.org/10.1175/1520-0442(1991)004<0269:tiomts>2.0.co;2)
- Chang, Y.-L., & Oey, L.-Y. (2011). Interannual and seasonal variations of Kuroshio transport east of Taiwan inferred from 29 years of tide-gauge data. *Geophysical Research Letters*, 38, L08603. <https://doi.org/10.1029/2011GL047062>
- Chen, X., Qiu, B., Chen, S., Cheng, X., & Qi, Y. (2018). Interannual modulations of the 50-day oscillations in the Celebes Sea: Dynamics and impact. *Journal of Geophysical Research*, 123, 4666–4679. <https://doi.org/10.1029/2018JC013960>
- Chen, X., Qiu, B., Chen, S., Qi, Y., & Du, Y. (2015). Seasonal eddy kinetic energy modulations along the North Equatorial Countercurrent in the western Pacific. *Journal of Geophysical Research*, 120, 6351–6362. <https://doi.org/10.1002/2015JC011054>
- Chen, X., Qiu, B., Du, Y., Chen, S., & Qi, Y. (2016). Interannual and interdecadal variability of the North Equatorial Countercurrent in the Western Pacific. *Journal of Geophysical Research: Oceans*, 121, 7743–7758. <https://doi.org/10.1002/2016JC012190>
- Chen, Z., & Wu, L. (2011). Dynamics of the seasonal variation of the North Equatorial Current bifurcation. *Journal of Geophysical Research*, 116, C02018. <https://doi.org/10.1029/2010JC006664>
- Dee, D. P., Uppala, S. M., Simmons, A. J., Berrisford, P., Polis, P., & Kobayashi, S. (2011). The ERA-Interim reanalysis: Configuration and performance of the data assimilation system. *Quarterly Journal of the Royal Meteorological Society*, 137, 553–597. <https://doi.org/10.1002/qj.828>
- Duan, J., Li, Y., Wang, F., & Chen, Z. (2019a). Decadal variations of the Mindanao Current during 1960–2010. *Journal of Geophysical Research*, 124, 2660–2678. <https://doi.org/10.1029/2019JC014975>
- Duan, J., Li, Y., Wang, F., & Chen, Z. (2019b). Multidecadal change of the Mindanao Current: Is there a robust trend? *Geophysical Research Letters*, 46, 6755–6764. <https://doi.org/10.1029/2019gl083090>
- England, M., McGregor, S., Spence, P., Meehl, G. A., Timmermann, A., Cai, W., et al. (2014). Recent intensification of wind-driven circulation in the Pacific and the ongoing warming hiatus. *Nature Climate Change*, 4, 222–227. <https://doi.org/10.1038/nclimate2106>
- Gordon, A. L., & Fine, R. A. (1996). Pathways of the water between the Pacific and Indian oceans in the Indonesian seas. *Nature*, 379, 146–149. <https://doi.org/10.1038/379146a0>
- Heron, S. F., Metzger, E. J., & Skirving, W. J. (2006). Seasonal variations of the ocean surface circulation in the vicinity of Palau. *Journal of Oceanography*, 62, 413–426. <https://doi.org/10.1007/s10872-006-0065-3>
- Hsin, Y.-C., & Qiu, B. (2012). Seasonal fluctuations of the surface North Equatorial Countercurrent (NECC) across the Pacific basin. *Journal of Geophysical Research*, 117, C06001. <https://doi.org/10.1029/2011JC007794>
- Hu, D., Wu, L., Cai, W., Gupta, A. S., Ganachaud, A., Qiu, B., et al. (2015). Pacific western boundary currents and their roles in climate. *Nature*, 522, 299–308. <https://doi.org/10.1038/nature14504>
- Hu, S., Lu, X., Li, S., Wang, F., Guan, C., Hu, D., et al. (2021). Multi-decadal trends in the tropical Pacific western boundary currents retrieved from historical hydrological observations. *Science China Earth Sciences*, 64(4), 600–610. <https://doi.org/10.1007/s11430-020-9703-4>
- Kashino, Y., Atmadipoera, A., Kuroda, Y., & Lukijanto (2013). Observed features of the Halmahera and Mindanao Eddies. *Journal of Geophysical Research*, 118, 6543–6560. <https://doi.org/10.1002/2013JC009207>
- Kashino, Y., Firing, E., Hacker, P., Sulaiman, A., & Lukijanto (2001). Currents in the Celebes and Maluku Seas. *Geophysical Research Letters*, 28, 1263–1266. <https://doi.org/10.1029/2000gl011630>
- Kashino, Y., Ishida, A., & Kuroda, Y. (2005). Variability of the Mindanao Current: Mooring observation results. *Geophysical Research Letters*, 32, L18611. <https://doi.org/10.1029/2005GL023880>
- Kawabe, M. (1995). Variation of current path, velocity, and volume transport of the Kuroshio in relation with the large meander. *Journal of Physical Oceanography*, 25, 3103–3117. [https://doi.org/10.1175/1520-0485\(1995\)025<3103:vocpva>2.0.co;2](https://doi.org/10.1175/1520-0485(1995)025<3103:vocpva>2.0.co;2)
- Kim, Y. Y., Qu, T., Jensen, T., Miyama, T., Mitsudera, H., Kang, H.-W., & Ishida, A. (2004). Seasonal and interannual variations of the North Equatorial Current bifurcation in a high-resolution OGCM. *Journal of Geophysical Research*, 109, C03040. <https://doi.org/10.1029/2003JC002013>
- Kosaka, Y., & Xie, S.-P. (2013). Recent global-warming hiatus tied to equatorial Pacific surface cooling. *Nature*, 501, 403–407. <https://doi.org/10.1038/nature12534>
- Kucharski, F., Kang, I. S., Farneti, R., & Feudale, L. (2011). Tropical Pacific response to 20th century Atlantic warming. *Geophysical Research Letters*, 38, L03702. <https://doi.org/10.1029/2010gl046248>
- Lukas, R. (1988). Interannual fluctuations of the Mindanao Current inferred from sea level. *Journal of Geophysical Research*, 93, 6744–6748. <https://doi.org/10.1029/jc093ic06p06744>
- Lukas, R., Firing, E., Hacker, P., Richardson, P. L., Collins, C. A., Fine, R. A., & Gammon, R. (1991). Observations of the Mindanao Current during the Western Equatorial Pacific Ocean circulation study. *Journal of Geophysical Research*, 96, 7089–7104. <https://doi.org/10.1029/91jc00062>
- Marshall, J. C., Adcroft, A., Hill, C., Perelman, L., & Heisey, C. (1997). A finite-volume, incompressible Navier Stokes model for studies of the ocean on parallel computers. *Journal of Geophysical Research*, 102, 5753–5766. <https://doi.org/10.1029/96jc02775>
- Masumoto, Y., & Yamagata, T. (1991). Response of the western tropical Pacific of the Asian winter Monsoon: The generation of the Mindanao Dome. *Journal of Physical Oceanography*, 21, 1386–1398. [https://doi.org/10.1175/1520-0485\(1991\)021<1386:rotwtp>2.0.co;2](https://doi.org/10.1175/1520-0485(1991)021<1386:rotwtp>2.0.co;2)
- Meehl, G. A. (1987). The annual cycle and interannual variability in the tropical Pacific and Indian Ocean regions. *Monthly Weather Review*, 115, 17–50. [https://doi.org/10.1175/1520-0493\(1987\)115<0027:tacaiv>2.0.co;2](https://doi.org/10.1175/1520-0493(1987)115<0027:tacaiv>2.0.co;2)
- Menemenlis, D., Fukumori, I., & Lee, T. (2005). Using Green's functions to calibrate an ocean general circulation model. *Monthly Weather Review*, 133(5), 1224–1240. <https://doi.org/10.1175/MWR2912.1>
- Merrifield, M. A. (2011). A shift in western tropical Pacific sea level trends during the 1990s. *Journal of Climate*, 24, 4126–4318.
- Qiu, B., & Chen, S. (2010). Interannual-to-decadal variability in the bifurcation of the North Equatorial Current off the Philippines. *Journal of Physical Oceanography*, 40, 2525–2538. <https://doi.org/10.1175/2010jp04462.1>
- Qiu, B., & Chen, S. (2012). Multi-decadal sea level and gyre circulation variability in the northwestern tropical Pacific Ocean. *Journal of Physical Oceanography*, 42, 193–206. <https://doi.org/10.1175/jpo-d-11-061.1>
- Qiu, B., & Lukas, R. (1996). Seasonal and interannual variability of the North Equatorial Current. *Journal of Geophysical Research*, 101(C5), 12315–12330. <https://doi.org/10.1029/95jc03204>
- Qiu, B., Mao, M., & Kashino, Y. (1999). Intraseasonal variability in the Indo-Pacific Throughflow and the regions surrounding the Indonesian Seas. *Journal of Physical Oceanography*, 29, 1599–1618. [https://doi.org/10.1175/1520-0485\(1999\)029<1599:ivitip>2.0.co;2](https://doi.org/10.1175/1520-0485(1999)029<1599:ivitip>2.0.co;2)

- Qiu, B., Rudnick, D. L., Cerveckei, I., Cornuelle, B. D., Chen, S., Schonau, M. C., et al. (2015). The Pacific North Equatorial Current: New insights from the Origins of the Kuroshio and Mindanao Currents (OKMC) project. *Oceanography*, 28(4), 24–33. <https://doi.org/10.5670/oceanog.2015.78>
- Rio, M. H., Guinehut, S., & Larnicol, G. (2011). New CNESCLS09 global mean dynamic topography computed from the combination of GRACE data, altimetry, and in situ measurements. *Journal of Geophysical Research*, 116, C07018. <https://doi.org/10.1029/2010JC006505>
- Schönaue, M. C., & Rudnick, D. L. (2017). Mindanao Current and Undercurrent: Thermohaline structure and transport from repeat glider observations. *Journal of Physical Oceanography*, 47, 2055–2075.
- Schönaue, M. C., Rudnick, D. L., Cerveckei, I., Gopalakrishnan, G., Cornuelle, B. D., McClean, J. L., & Qiu, B. (2015). The Mindanao Current: Mean structure and connectivity. *Oceanography*, 28(4), 34–45. <https://doi.org/10.5670/oceanog.2015.79>
- Tokunaga, H., Xie, S.-P., Deser, C., Kosaka, Y., & Okumura, Y. M. (2012). Slowdown of the Walker circulation driven by tropical Indo-Pacific warming. *Nature*, 491, 439–443. <https://doi.org/10.1038/nature11576>
- Torrence, C., & Compo, G. P. (1997). A practical guide to wavelet analysis. *Bulletin of the American Meteorological Society*, 79, 61–78.
- Tozuka, T., Kagimoto, T., Masumoto, Y., & Yamagata, T. (2002). Simulated multiscale variations in the western tropical Pacific: The Mindanao Dome revisited. *Journal of Physical Oceanography*, 32, 1338–1359. [https://doi.org/10.1175/1520-0485\(2002\)032<1338:smvitw>2.0.co;2](https://doi.org/10.1175/1520-0485(2002)032<1338:smvitw>2.0.co;2)
- Vecchi, G. A., Soden, B. J., Wittenberg, A. T., Held, I. M., Leetmaa, A., & Harrison, M. J. (2006). Weakening of tropical Pacific atmospheric circulation due to anthropogenic forcing. *Nature*, 441, 73–76. <https://doi.org/10.1038/nature04744>
- Wijffels, S., Firing, E., & Toole, J. (1995). The mean structure and variability of the Mindanao Current at 8°N. *Journal of Geophysical Research*, 100(C9), 18421–18435. <https://doi.org/10.1029/95jc01347>
- Woodworth, P., & Player, R. (2003). The permanent service for mean sea level: An update to the 21st Century. *Journal of Coastal Research*, 19, 287–295.
- Wu, C.-R., Lin, Y.-F., & Qiu, B. (2019). Impact of the Atlantic multidecadal oscillation on the Pacific North Equatorial Current bifurcation. *Scientific Reports*, 9, 2162. <https://doi.org/10.1038/s41598-019-38479-w>
- Wunsch, C., Heimbach, P., Ponte, R., & Fukumori, I. (2009). The global general circulation of the ocean estimated from the ECCO-consortium. *Oceanography*, 22(2), 88–103. <https://doi.org/10.5670/oceanog.2009.41>
- Yamaguchi, R., & Suga, T. (2019). Trend and variability in global upper ocean stratification since the 1960s. *Journal of Geophysical Research*, 124, 8933–8948. <https://doi.org/10.1029/2019JC015439>
- Yasunari, T. (1989). A possible link of the QBOs between the stratosphere, troposphere and sea surface temperature in the tropics. *Journal of the Meteorological Society of Japan. Ser. II*, 67, 483–493. https://doi.org/10.2151/jmsj1965.67.3_483
- Zhang, L., Hu, D., Hu, S., Wang, F., Wang, F., & Yuan, D. (2014). Mindanao Current/Undercurrent measured by a subsurface mooring. *Journal of Geophysical Research*, 119, 3617–3628. <https://doi.org/10.1002/2013JC009693>
- Zhao, J., Li, Y., & Wang, F. (2013). Dynamical responses of the west Pacific North Equatorial Countercurrent (NECC) system to El Niño events. *Journal of Geophysical Research: Oceans*, 118, 2828–2844. <https://doi.org/10.1002/jgrc.20196>